Formation of stable products from cluster–cluster collisions

2007 J. Phys.: Condens. Matter 19 346204

(http://iopscience.iop.org/0953-8984/19/34/346204)

IOP PUBLISHING JOURNAL OF PHYSICS: CONDENSED MATTER

J. Phys.: Condens. Matter **19** (2007) 346204 (12pp) doi:10.1088/0953-8984/19/34/346204

Formation of stable products from cluster–cluster collisions

Denitsa Alamanova[1], **Valeri G Grigoryan and Michael Springborg**

Physical and Theoretical Chemistry, University of Saarland, 66123 Saarbrücken, Germany

E-mail: deni@springborg.pc.uni-sb.de, vg.grigoryan@mx.uni-saarland.de and m.springborg@mx.uni-saarland.de

Received 9 May 2007, in final form 17 June 2007
Published 20 July 2007
Online at stacks.iop.org/JPhysCM/19/346204

Abstract

The formation of stable products from copper cluster–cluster collisions is investigated by using classical molecular-dynamics simulations in combination with an embedded-atom potential. The dependence of the product clusters on impact energy, relative orientation of the clusters, and size of the clusters is studied. The structures and total energies of the product clusters are analysed and compared with those of the colliding clusters before impact. These results, together with the internal temperature, are used in obtaining an increased understanding of cluster fusion processes.

(Some figures in this article are in colour only in the electronic version)

1. Introduction

Collision processes are an important ingredient in nuclear and cluster physics [1, 2]. For instance, cluster–cluster collisions provide understanding of the formation of macroscopic aggregates and cluster molecules, and of collision-induced dissociations, and vibrational energy transfer between two clusters (see, e.g., [3]).

From a theoretical point of view, it is most convenient to study such processes by means of molecular-dynamics (MD) simulations. Then, there are two fundamentally different approaches, i.e., *adiabatic* cluster collisions, in which the reaction channels involve only vibrational and rotational excitations, and *nonadiabatic* collisions, in which electronic effects are also included [4]. Much interest is paid to the adiabatic collisions, where larger clusters can be studied for a longer simulation time by combining classical molecular dynamics with (semi-) empirical potentials for the description of the interatomic interactions, whereas nonadiabatic simulations like the quantum molecular dynamics (QMD) [5, 6], employing different density functionals, have their limitations, including shorter simulation times and smaller systems.

Experimentally, small copper particles, Cu_N, have an unusual electrochemical stability [7], which makes them attractive candidates for electrocatalysts. In order to identify the sizes of the

[1] Author to whom any correspondence should be addressed.

particularly stable clusters, Krückeberg and co-workers [8] studied the decay pathways and dissociation energies of small singly and doubly charged copper clusters by using the multiple-collision induced dissociation method. For singly charged clusters, an odd–even oscillation in the dissociation energy was observed, with particularly large values for $N = 3, 9, 15$, and 21, suggesting electronic shell closures for $N = 2, 8, 14$, and 20.

On the other hand, theoretical studies of collision processes between copper clusters have not been presented so far, whereas more studies on sodium clusters have been reported. Thus, such processes between magic sodium clusters with $N = 2, 8, 20$, and 40 atoms were studied by Schmitt and co-workers [12] using a two-centre jellium model for the ionic cores. The energetic stability of cluster molecules (i.e., $Na_{N_1}Na_{N_2}$ molecules resulting from $Na_{N_1} + Na_{N_2}$ collision processes and containing the largely unchanged initial entities), as well as the main reaction channels of the cluster–cluster collisions were studied theoretically by Seifert *et al* [10, 11] by using MD calculations combined with a density-functional formalism within the local-density approximation (LDA). According to this study, the Na_9Na_9 molecule formed in collisions between two Na_9 clusters has binding energy close to that of the magic Na_{18} cluster, while the Na_8Na_8 molecule is unstable. A study concerning the thermodynamical stability of cluster dimers [9] confirmed that the latter cluster molecule was not a stable structure except for the special situation in which the structure resulting from the collision was that of the stable Na_{16} cluster. This was also confirmed by Häkkinen and Manninen [13] using *ab initio* molecular dynamics. The same issue was further investigated by Zhang *et al* [14] using a tight-binding approximation, in which, in addition, the possibility of formation of the $Na_{19}Na_{19}$ and $Na_{20}Na_{20}$ cluster dimers was studied.

The purpose of the present work is to study collision processes between two Cu clusters with N_1 and N_2 atoms for low impact energies. Special emphasis is put on the characterization of the products as a function of impact energy and size of the colliding clusters. In particular, we shall explore whether the product resembles either the initial clusters, Cu_{N_1} and Cu_{N_2}, or the most stable larger $Cu_{N_1+N_2}$ cluster. In the former case, one may consider the product as being a cluster molecule, whereas the latter case corresponds to a fusion process. A study with a similar aim was recently presented by Rogan *et al* [15], who investigated collision processes between small gold clusters using a parameterized potential for the interatomic interactions similar to the one we shall use, i.e., the Voter and Chen [16, 17] version of the embedded-atom method [18]. Rogan *et al* [15] varied the collision energy and the impact parameter in order to cover the complete fusion, scattering, and fragmentation regimes. Here, however, we are interested in fusion processes in the low collision-energy range.

2. Method and computational scheme

In this work we simulated the collision processes between different magic and non-magic clusters using the Voter–Chen version [16, 17] of the embedded-atom method (EAM) in combination with a classical molecular-dynamics scheme.

According to the EAM method the total energy of the system is written as a sum over atomic energies,

$$E_{\text{tot}} = \sum_{i}^{N} E_i \tag{1}$$

with

$$E_i = F_i(\rho_i^h) + \tfrac{1}{2}\sum_{j\neq i}\phi_{ij}(r_{ij}). \tag{2}$$

Table 1. The total energies and symmetries of the isolated substrate clusters used in this study.

No. 1	No. 2	Prod.	Energy 1 (eV)	Energy 2 (eV)	Sym 1	Sym 2
6	6	12	−12.81	−12.81	O_h	O_h
6	7	13	−12.81	−15.54	O_h	D_{5h}
9	9	18	−21.01	−21.01	C_{2v}	C_{2v}
9	10	19	−21.01	−23.88	C_{2v}	C_{3v}
13	13	26	−33.49	−33.49	I_h	I_h
14	14	28	−35.94	−35.94	C_{3v}	C_{3v}
19	19	38	−50.96	−50.96	D_{5h}	D_{5h}
23	23	46	−62.78	−62.78	D_{3h}	D_{3h}
23	26	49	−62.78	−71.61	D_{3h}	T_d
14	57	71	−35.94	−167.98	C_{3v}	C_5

The first term is the so-called embedding energy, which is obtained by considering each atom as an impurity embedded into a host provided by the rest of the atoms. The second term describes electron–electron interactions and is represented in terms of short-ranged pair potentials. The local density at site i is assumed being a superposition of atomic electron densities,

$$\rho_i^h = \sum_{j\,(\neq i)} \rho_i^{\mathrm{a}}(r_{ij}) \tag{3}$$

where $\rho_i^{\mathrm{a}}(r_{ij})$ is the spherically averaged atomic electron density provided by atom j at the distance r_{ij}. Notice that compared to non-interacting, neutral atoms, E_{tot} is negative for stable structures. In our study we use the original expression by Voter and Chen for the embedding energy and pair potentials.

The optimized structures of the isolated clusters are taken from our previous work [19, 20], in which we studied the structure and energetics of small and middle-sized nickel, copper, and gold clusters. There, we used an unbiased approach in determining the structure of the global total-energy minima for clusters with up to 150 atoms. The EAM methods describe successfully the properties of crystals, phonons, and interfaces, and in our work we found that the EAM also describes well the properties of small clusters (with Au being a possible exception). Therefore, we are confident of using this approach for collision processes between small Cu clusters.

For the sake of completeness we show the structures of the clusters used in the present study in table 1 and figure 1.

In the simulation of the reaction paths we use classical constant-energy molecular dynamics in order to investigate larger structures over a longer simulation time. The Newtonian equations of motion are integrated by using the velocity Verlet algorithm with time steps of 1×10^{-15} s. The integration time in most of the simulations was 35 ps, while for the larger clusters some of the calculations were extended up to 50 ps. In order to identify the products of the collision processes, the simulations include a final simulated-annealing period of 5 ps. This period is also included as a means of simulating cooling processes in which the colliding clusters lose their initial kinetic energy through collisions processes with surrounding gas molecules, walls, etc.

We simulated the collision events between various magic and nonmagic copper clusters at centre-of-mass incident energies of $E = 0.0$, 0.038, 0.1, 0.3, and 0.5 eV/atom, and chose in all simulations the impact parameter $b = 0$, as our study is concerned entirely with possible fusion processes between the clusters. In most cases the initial orientation of the clusters contained parallel principal axes of inertia, although some additional calculations with different relative orientations were also performed. The initial structure was chosen so that the atoms of the two

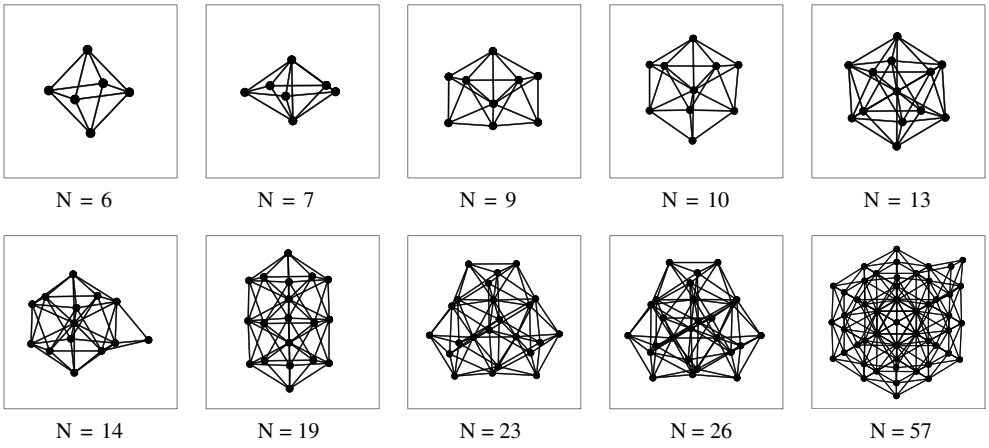

Figure 1. The initial structures of the copper clusters studied in the collision processes.

impacting clusters just start to interact with each other, i.e., the smallest distance between atoms of the two clusters is initially 2–3 Å.

3. Results and discussion

We shall split the discussion of our results into three parts, i.e., energetic properties, structural properties, and internal temperature.

3.1. Energetic properties

In all calculations, we find that the total energy of the final product of the $Cu_{N_1} + Cu_{N_2}$ collision process is very close to that of the global-minimum structure of the $Cu_{N_1+N_2}$ cluster. This is illustrated in figure 2. It is seen that there is an overall tendency for the total energy of the final product to decrease as a function of increasing impact energy, although smaller deviations occur. This overall decrease can be explained through the total-energy hypersurface that has an essentially exponentially growing number of local minima with cluster size so that it becomes very likely that the product cluster gets trapped in not the global, but in an energetically higher-lying local total-energy minimum.

An interesting exception is that of $(N_1, N_2) = (6, 7)$, which corresponds to the lowest curve in the figure. In this case, the relative total energy shows the largest deviations from that of the globally optimized structure with $N = 13$ atoms, in particular for an impact energy around 0.3 eV/atom. The Cu_{13} cluster is particularly stable, having icosahedral symmetry, and it is possible that this structure corresponds to a global total-energy minimum with a narrow basin, i.e., even smaller deviations from this structure will lead to structures of other local total-energy minima. In that case, it is unlikely that the structures that result from a collision process will relax to the icosahedron.

It turned out that longer simulation times in some cases lead to lower total energies of the products, i.e., to different structures. At a non-zero temperature the systems have the possibility to overcome energy barriers between different local total-energy minima, explaining our finding. Moreover, this implies that in experiment slow and fast cooling rates may lead to different products.

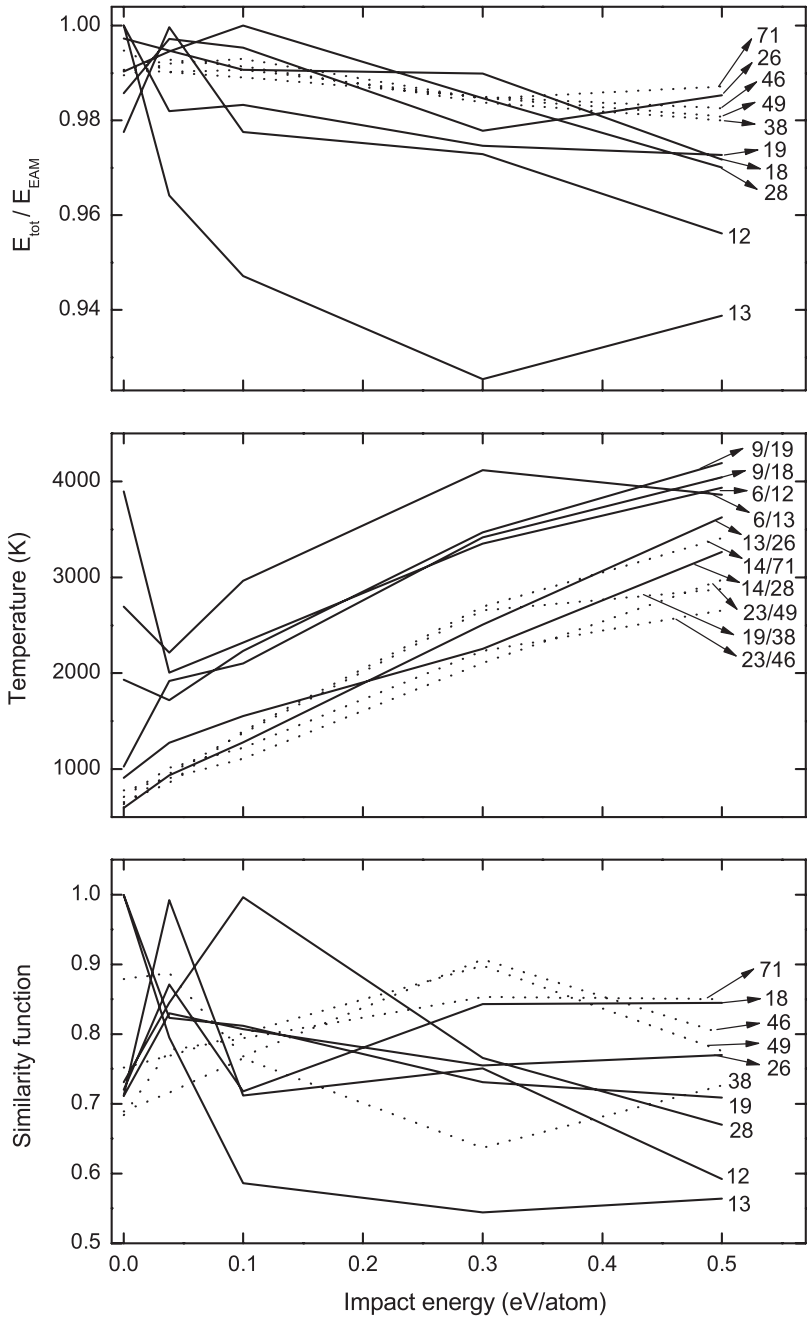

Figure 2. Various properties quantifying the end product of the $Cu_{N_1} + Cu_{N_2}$ collision process compared to the cluster with $N = N_1 + N_2$ atoms. The top panel shows the total energy of the final product ($E_{\rm tot}$) relative to that of the Cu_N cluster ($E_{\rm EAM}$), whereas the middle panel shows the maximal internal temperature of some of the reacting clusters. Here, the labels on the right show N_1/N or N_2/N. The lowest panel gives the similarity function, quantifying whether the structure of the final product of the collision resembles the structure of the global total-energy minimum for the Cu_N cluster. The labels show N. In each panel, the solid curves represent the results for $N \leqslant 28$ and the dashed curves those for $N \geqslant 38$.

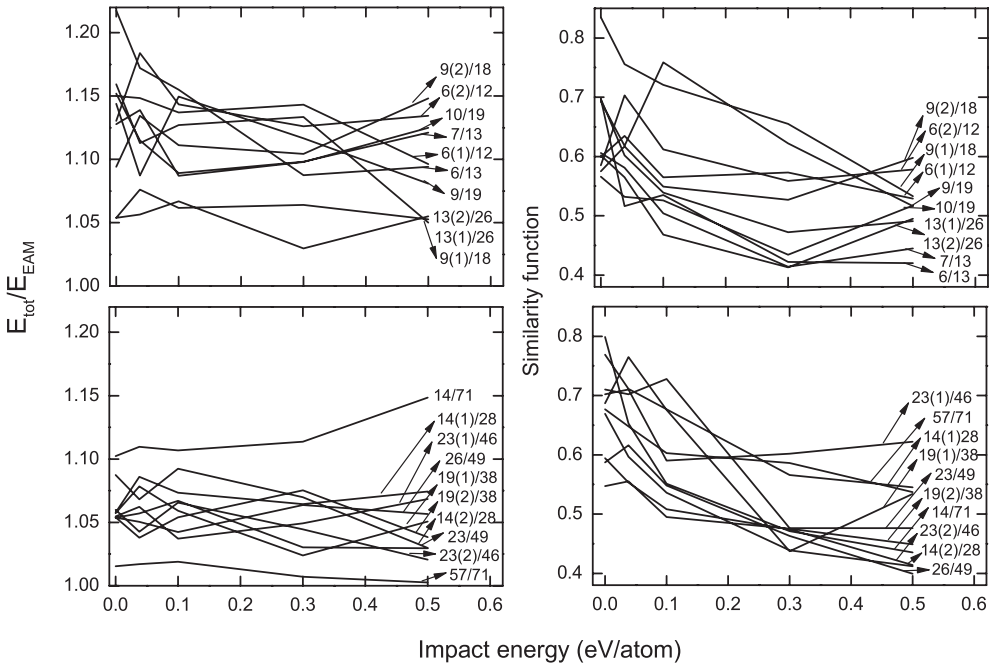

Figure 3. Various properties used in comparing the final and initial structures of the Cu_{N_1} and Cu_{N_2} clusters. The left panels show the total energy of the final structures (E_{tot}) relative to that of the initial one (E_{EAM}) for product clusters with fewer than 26 (top) and more than 26 (bottom) atoms. In the right panels we compare the structures themselves using the similarity functions. The results are presented similarly to the left panels; for details see the text. The labels show N_1/N or N_2/N ($N = N_1 + N_2$).

We may use equations (1) and (2) in analysing the energy distribution of the final products. Equation (2) allows us to ascribe to each atom a certain part of the total energy, and by adding the contributions from the N_1 or N_2 atoms of the colliding clusters after the collision, we can split the total energy of the final structure into contributions from the two initial clusters. Finally, these can be compared with the total energies of the two clusters before they start interacting. The results are shown in the left panels in figure 3. Since the atoms of the final structures interact with more atoms, the total energy goes down (becomes more negative), i.e., the relative total energies are in all cases above 1. Moreover, the smallest part ($N_1 = 14$) of the largest system ($N_1 + N_2 = 71$) is for that reason the system for which the relative total energy is the largest. Beyond these findings, that merely are a result of our approach of analysing the results, the figure indicates an overall decrease in the relative total energy as a function of impact energy with some deviations for the absolutely smallest impact energies. This is a confirmation of the findings above that for the larger impact energies the systems get trapped in energetically higher-lying structures.

3.2. Structural properties

For an impact energy of 0.0 eV/atom, the simulations for which the main axes of the colliding clusters were aligned led to the following product structures. For $N_1 = N_2 = 6$ the final structure constituted of two octahedra with a common side and two additional atoms lying next to each other on one of the sides. It can be considered as a 'double octahedron' bridged by two

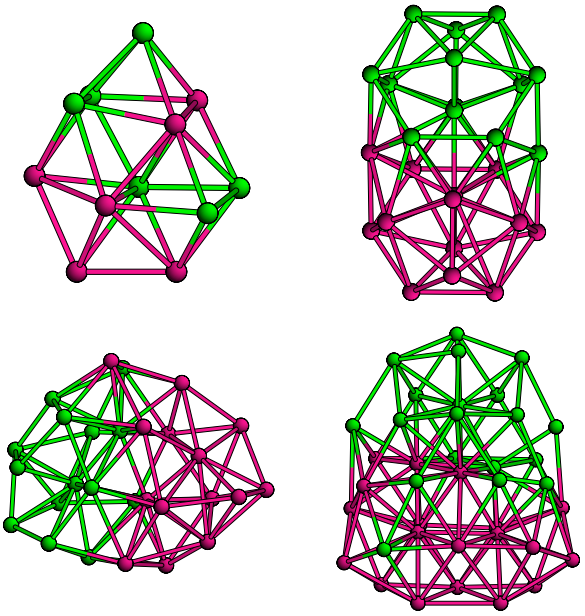

Figure 4. The product of a $Cu_{N_1} + Cu_{N_2}$ collision process for zero impact energy. (N_1, N_2) equals (top, left) (6, 6), (top, right) (13, 13), (bottom, left) (14, 14), and (bottom, right) (19, 19).

atoms. The $N_1 = N_2 = 13$ system has a symmetrical, oblate shape suggesting the formation of a dimer. This cluster possesses the higher D_{3d} symmetry, in contrast to the low-symmetrical $N_1 = N_2 = 6$ and $N_1 = N_2 = 19$ cases of C_1 symmetry. On the other hand, the $N_1 = N_2 = 14$ system (with D_2 symmetry) contains elements of tetrahedral symmetry and can be considered a fusion product. These four systems are shown in figure 4.

Repeating the simulation for the $N_1 = N_2 = 6$ system, but for other relative spatial orientations, the structure of the global total-energy minimum for Cu_{12} was found at impact energies of 0.038 eV/atom and higher. The formation of a dimer molecule was not observed in any of the simulations for this cluster size. On the other hand, for the $Cu_{13} + Cu_{13}$ interaction at an impact energy of 0.0 eV and with aligned main axes, a stable cluster dimer was formed for around 2.45 ps simulation time, at which time a final rearrangement led to the highly symmetrical product Cu_{26}. For the $Cu_{19} + Cu_{19}$ and $Cu_{14} + Cu_{14}$ systems short-living dimers were observed for the first 1.75 ps and 1.4 ps of the simulations, respectively.

In figure 5 we show the $Cu_{13}Cu_{13}$ dimer structures at different stages of the simulation. When rotating one of the Cu_{13} colliding clusters by 90° about an axis perpendicular to the collision direction, a dimer formation was not observed even at the beginning of the collision, but the clusters rapidly fused, resulting in a low-symmetry product. The same behaviour was observed for the simulations leading to the Cu_{28} and Cu_{38} products. Therefore, whether dimers are found is strongly dependent on the initial cluster orientation.

Calculations for colliding clusters with 4, 7, and 10 atoms all led to dimer formations at different stages of the simulations. For $Cu_7 + Cu_7$, the dimer existed between 0.7 and 2.1 ps, the $Cu_{10}Cu_{10}$ molecule lived for 1.2 ps, and, finally, the Cu_4Cu_4 dimer turned out to be highly stable, having a lifetime of 8.4 ps. At the end of the simulations the $Cu_4 + Cu_4$ system had reached the geometry of the global total-energy minimum for $N = 8$ whereas the Cu_{14} and Cu_{20} clusters had low-symmetry structures, corresponding to higher-lying isomers for those cluster sizes. The fact that the number of local total-energy minima grows essentially exponentially

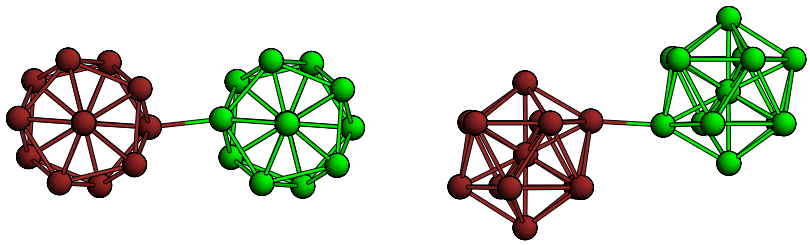

t = 1225fs (side and top view)

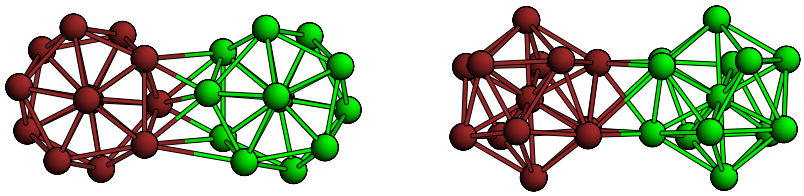

t = 2450fs (side and top view)

Figure 5. The formation of a $Cu_{13}Cu_{13}$ dimer.

with the size of the system can explain why the collisions for the larger systems do not result in the structures of the global total-energy minima.

In order to check the influence of the relative orientation of the clusters, we performed calculations on the same set of clusters but with other initial orientations of the colliding particles. The results did not indicate any dimer formation, again implying that the outcome of the collision processes depends very sensitively on all details of the process.

We shall now study how the structural properties of the collision product depend on the properties of the individual properties of the colliding clusters. In particular, we shall explore whether both, or at least one, of the colliding clusters experience(s) significant structural changes, i.e., whether one may talk about a 'harder' and a 'softer' cluster. To this end we shall use the concept of similarity functions [20]. These can be used also to quantify to which extent the products are more fcc- or icosahedral-like.

When comparing two different structures of N atoms, we calculate for each atom of each of the two structures its distance to the centre of mass of the system of interest. These two sets of so-called radial distances $\{r_n\}$ and $\{r'_n\}$ are sorted. Then, from

$$q = \left[\frac{1}{N}\sum_{n=1}^{N}(r_n - r'_n)^2\right]^{1/2}, \tag{4}$$

the similarity function is defined as

$$S = \frac{1}{1 + q/u_l} \tag{5}$$

($u_l = 1$ Å), which approaches 1 (0) for very similar (different) structures.

For the $Cu_{N_1} + Cu_{N_2}$ collision process we compared the final structure with the two initial structures of the non-interacting clusters. We considered all subsets of N_1 (N_2) atoms of the product cluster and compared each of those with the isolated cluster of N_1 (N_2) atoms.

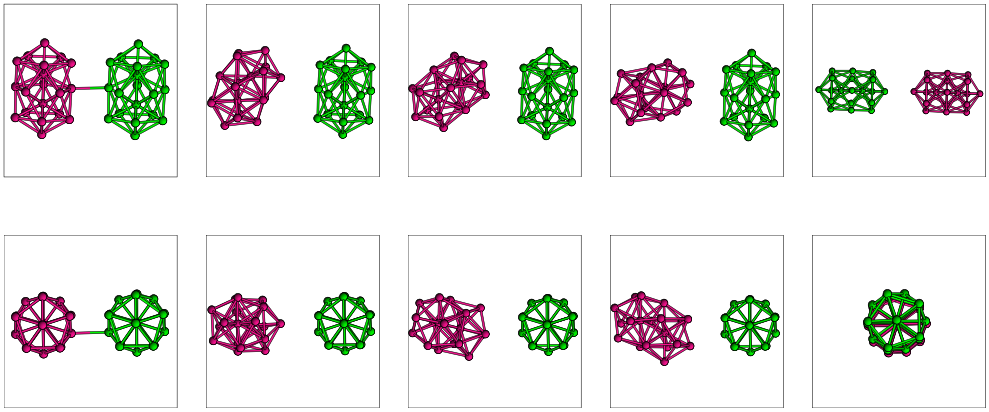

Figure 6. Side and top view of the initial orientations of the two interacting Cu_{19} clusters. From left to the right the impact angle corresponds to 0°, 30°, 60°, and 90°. The configuration in which the principal axes of inertia of both clusters are aligned (right) is also considered.

However, the results (not shown) did not indicate a correlation between size or impact energy on the one hand and similarity function on the other. Thus, although the total energy of the products in general decreases as a function of impact energy, see the upper panel in figure 2, this does not imply that the structures of the clusters become increasingly different from those of the colliding clusters before impact.

Instead we compare the final structure of the $Cu_{N_1} + Cu_{N_2}$ collision process with the structure of the global total-energy minimum of the Cu_N ($N = N_1 + N_2$) cluster. For a larger impact energy, the atoms of the colliding clusters may be able to avoid getting trapped in local total-energy minima and, therefore, will be able to obtain the structure of the global total-energy minimum. Alternatively, for smaller impact energies it is possible that the clusters do not break up into smaller fragments that are not able to relax to the structure of the global total-energy minimum. The lowest panel in figure 2 shows the results. There is at most a weak tendency for a decreasing similarity function with increasing impact energy. Moreover, for slightly larger impact energies the smaller clusters tend to obtain structures that are most different from those of the global total-energy minima, although this quantitative difference between smaller and larger systems might be related to our precise definition of our descriptors.

When using the similarity functions in comparing the product clusters and different *fcc* and *icosahedral* structures (not shown) fairly low values are found. This is in agreement with the observation that the structures of the global total-energy minima in this size range only for few special sizes (e.g., $N = 13$ for which an icosahedron is found) resemble *fcc* of *icosahedral* fragments.

When comparing the final structures of the N_1 and N_2 atoms with those of the initial structures (using the similarity functions above) we see, see the right panels in figure 3, that in general the structures become increasingly different from the initial structures when increasing the impact energy. But from the discussion above it is clear that this change is not accompanied with a trend towards more stable final structures.

Finally, we shall study the structure and the overall shape of a collision process by varying the relative orientation of the two colliding clusters as well as the impact energy. We shall consider the single case of $N_1 = N_2 = 19$ shown at figure 6.

For a structure with N atoms we calculate the 3×3 matrix with the components $\sum_{i=1}^{N} s_i t_i$ with s_i and t_i being the x, y, or z component of the ith atom relative to the centre of mass.

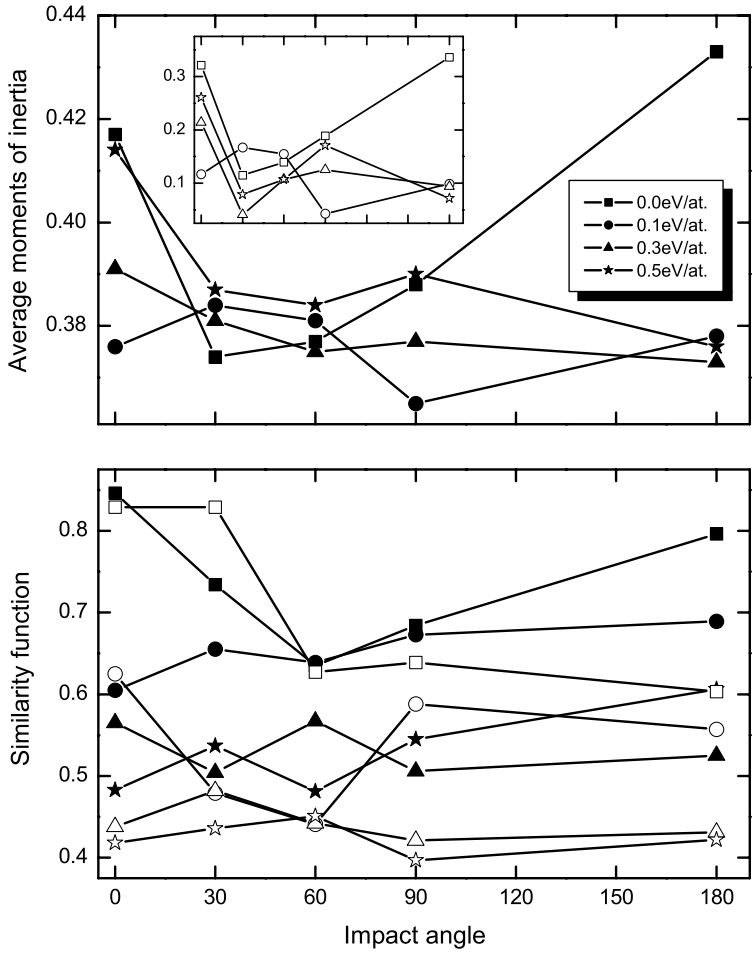

Figure 7. Various properties used in comparing the final structures of the $Cu_{19} + Cu_{19}$ collision process. The top panel shows quantities related to the overall shape. Here, the average value of the eigenvalues of the matrix containing $\sum_i s_i t_i$ is shown (for details, see the text) and the inset shows the largest difference of those. In the bottom panel the similarity function between the initial and final structures of the colliding clusters is shown. Squares, circles, triangles, and stars mark results for impact energies of 0.0, 0.1, 0.3, and 0.5 eV/atom, respectively. Here, open and closed symbols are used in distinguishing the two clusters.

The eigenvalues of this matrix give information on the overall shape. In particular, compact structures have a small average value and spherical systems have three identical values.

In the upper panel in figure 7 we show the results of this analysis. It is interesting to observe that for impact angles of 30° and 60° the overall shape depends only weakly on the impact energy. Moreover, situations can be identified (e.g., an impact angle of 30° and an impact energy of 0.3 eV/atom as well as an impact angle of 60° and an impact energy of 0.1 eV/atom) in which the product cluster is essentially spherical. On the other hand, for other impact angles (e.g., 0° and 180°) the final structure depends strongly on the impact energy.

Also when comparing the initial and final structure of the colliding clusters it becomes clear that the results depend sensitively on the impact angle. This is illustrated in the lower panel in figure 7.

3.3. Internal temperature

One interesting issue in connection with the behaviour of the colliding clusters is the variation of the internal temperatures of each cluster during the collision process. We define these as follows. For each of the two clusters we determine its centre of mass,

$$\vec{R}_{0,j} = \frac{1}{N_j} \sum_{i=1}^{N_j} \vec{R}_{i,j}, \tag{6}$$

where $\vec{R}_{i,j}$ is the position of the ith atom of the jth cluster and N_j is the number of atoms in the jth cluster. Subsequently, the internal temperature of the jth cluster, T_j, is defined as

$$\tfrac{3}{2} N_j k_B T_j = \tfrac{1}{2} m \sum_{i=1}^{N_j} \left[|\dot{\vec{R}}_{i,j}|^2 - |\dot{\vec{R}}_{0,j}|^2 \right] \tag{7}$$

where m is the mass of a Cu atom, k_B is the Boltzmann constant, and the dots represent time derivatives.

The highest internal temperatures that are reached in the collision processes are shown in the middle panel in figure 2, where each curve corresponds to the value for one of the two colliding clusters. The results show a clear difference between the smaller clusters with up to nine atoms and the larger ones. For three of the four cases including smaller clusters, the temperature possesses minima at 0.038 eV/atom impact energy, which, comparing to the zero impact energy, can be explained with the lower mobility of the cluster centre of masses of the latter, leading to a higher internal temperature. Moreover, except for the case of an impact energy of 0 eV/atom for the smallest structures, the relation between impact energy and temperature is almost linear for all clusters. However, again the case of $N = 13$ and an impact energy of 0.3 eV/atom is different, with a particularly high maximal internal temperature. The high internal temperature suggests that the atoms are moving much, which, therefore, may result in a final structure of an unusual low total energy, see figure 2.

4. Conclusions

We have studied collision processes between smaller copper clusters at different impact energies in order to find possible relations between the initial energies and the energetic and structural stability of the products. Our theoretical study was based on classical molecular-dynamics simulations in combination with the embedded atom potential for the description of interatomic interactions.

A main finding of our study is that with increasing impact energy the final products of the $Cu_{N_1} + Cu_{N_2}$ collision become increasingly different from the structure of the global total-energy minimum of the Cu_N ($N = N_1 + N_2$) cluster. The maximal internal temperature showed an essentially linear dependence on the impact energy, i.e., the atoms become increasingly mobile, which most likely is the reason for why the final structures of the collision processes depend sensitively on all parameters of the collision process, i.e., size of the clusters, impact energy, relative orientation, and impact parameter. In the present study we have demonstrated this with the exception of the dependence on the impact parameter that was not varied.

A further outcome of our study was the prediction of the possible formation of the cluster molecules Cu_4Cu_4, Cu_7Cu_7, $Cu_{10}Cu_{10}$, $Cu_{13}Cu_{13}$, $Cu_{14}Cu_{14}$, and $Cu_{19}Cu_{19}$ similar to the earlier findings for sodium clusters [14]. In all cases we have studied, the stability of the cluster molecules (including their lifetime) shows a strong dependence on the initial orientation of the clusters. For larger impact energies dimer formation was not observed.

The structural comparison between the product clusters and different fcc and icosahedral structures shows that all collision products have only marginal similarity with fcc-like and icosahedral-like structures.

In total, our results show that even at extremely well-defined experimental conditions, cluster–cluster collision experiments should be expected to lead to a broad spectrum of resulting structures. The most stable structures are obtained for low, although not almost vanishing, impact energies.

Acknowledgments

We gratefully acknowledge *Fonds der Chemischen Industrie* for very generous support. This work was supported by the SFB 277 of the University of Saarland and by the German Research Council (DFG) through project Sp439/14-1.

References

[1] Bock R 1980 *Heavy Ion Collisions* (Amsterdam: North-Holland)
[2] Bransden B H 1983 *Atomic Collision Theory* (Reading: Benjamin-Cummings)
[3] Andersen N *et al* 1988 *Phys. Rep.* **165** 1
Andersen N *et al* 1997 *Phys. Rep.* **278** 107
Andersen N *et al* 1997 *Phys. Rep.* **279** 251
[4] Saalmann U and Schmidt R 1998 *Phys. Rev. Lett.* **80** 3213
[5] Knospe O, Glotov A V, Seifert G and Schmidt R 1996 *J. Phys. B: At. Mol. Opt. Phys.* **29** 5163
[6] Schmidt R, Knospe O and Saalmann U 1997 *Nuovo Cimento* A **110** 1201
[7] Kolb D M, Engelmann G E and Ziegler J C 2000 *Angew. Chem. Int. Edn* **39** 1123
[8] Krückeberg S, Schweikhard L, Ziegler J, Dietrich G, Lützenkirchen K and Walther C 2001 *J. Phys. Chem.* **114** 2955
[9] Calvo F and Spiegelmann F 1996 *Phys. Rev.* B **54** 10949
[10] Schmidt R, Seifert G and Lutz H O 1991 *Phys. Lett.* A **158** 231
[11] Seifert G, Schmidt R and Lutz H O 1991 *Phys. Lett.* A **158** 237
[12] Schmitt U R, Engel E and Dreizler R M 1994 *Phys. Rev.* B **50** 14674
[13] Häkkinen H and Manninen M 1996 *Phys. Rev. Lett.* **76** 1599
[14] Zhang F S, Spiegelmann F, Suraud E, Frayssé V, Poteau R, Glowinski R and Chatelin F 1994 *Phys. Lett.* A **193** 75
[15] Rogan J, Ramírez R, Romero A H and Kiwi M 2004 *Eur. Phys. J.* D **28** 219
[16] Voter A F and Chen S P 1987 *Characterization of Defects in Materials* (*MRS Symposia Proc. No. 82*) ed R W Siegal, J R Weertman and R Sinclair (Pittsburgh, PA: Materials Research Society) p 175
[17] Voter A F 1995 *Intermetallic Compounds* vol 1, ed J H Westbrook and R L Fleischer (New York: Wiley) p 77
[18] Daw M S and Baskes M I 1983 *Phys. Rev. Lett.* **50** 1285
[19] Grigoryan V G, Alamanova D and Springborg M 2005 *Eur. Phys. J.* D **34** 187
[20] Grigoryan V G, Alamanova D and Springborg M 2006 *Phys. Rev.* B **73** 115415